

# Virtual and Physical Prototyping

ISSN: (Print) (Online) Journal homepage: [www.tandfonline.com/journals/nvpp20](http://www.tandfonline.com/journals/nvpp20)

## Multi-material and parameter-controllable stereolithography 3D printing of graded permittivity composites for high voltage insulators

Lipeng Zhong, Junxian Du, Yingwei Xi, Feng Wang, Linmei Wu, Jinyu Li, Min Tu, Xiaopeng Li & Guanghai Fei

**To cite this article:** Lipeng Zhong, Junxian Du, Yingwei Xi, Feng Wang, Linmei Wu, Jinyu Li, Min Tu, Xiaopeng Li & Guanghai Fei (2023) Multi-material and parameter-controllable stereolithography 3D printing of graded permittivity composites for high voltage insulators, *Virtual and Physical Prototyping*, 18:1, e2271447, DOI: [10.1080/17452759.2023.2271447](https://doi.org/10.1080/17452759.2023.2271447)

**To link to this article:** <https://doi.org/10.1080/17452759.2023.2271447>



© 2023 The Author(s). Published by Informa UK Limited, trading as Taylor & Francis Group



Published online: 24 Oct 2023.



Submit your article to this journal



Article views: 1266



View related articles



View Crossmark data



Citing articles: 4 View citing articles

# Multi-material and parameter-controllable stereolithography 3D printing of graded permittivity composites for high voltage insulators

Lipeng Zhong  <sup>a</sup>, Junxian Du <sup>a</sup>, Yingwei Xi <sup>a,b</sup>, Feng Wang <sup>a</sup>, Linmei Wu <sup>c</sup>, Jinyu Li <sup>d</sup>, Min Tu  <sup>e</sup>, Xiaopeng Li  <sup>f</sup> and Guanghai Fei  <sup>g</sup>

<sup>a</sup>College of Electrical and Information Engineering, Hunan University, Changsha, People's Republic of China; <sup>b</sup>Tangshan Power Supply Company, Tangshan, People's Republic of China; <sup>c</sup>College of Civil Engineering, Hunan Institute of Science and Technology, Yueyang, People's Republic of China; <sup>d</sup>China Electric Power Research Institute, Beijing, People's Republic of China; <sup>e</sup>2020 X-Lab, Shanghai Institute of Microsystem and Information Technology, Chinese Academy of Sciences, Shanghai, People's Republic of China; <sup>f</sup>School of Mechanical and Manufacturing Engineering, University of New South Wales (UNSW Sydney), Sydney, Australia; <sup>g</sup>Centre for Membrane Separations, Adsorption, Catalysis, and Spectroscopy (cMACS), KU Leuven, Leuven, Belgium

## ABSTRACT

Graded permittivity materials have gained significant attention due to their exceptional ability to regulate electric fields. Multi-material stereolithography (SLA) 3D printing has opened up new possibilities for creating such materials. However, conventional SLA printers typically generate graded material using fixed printing parameters and multiple feedstocks with limited differences, resulting in a constrained capacity for modulating the electric field distribution. To address this limitation, we have developed a multi-material, parameter-controllable SLA strategy, enabling us to assign varying printing parameters for each building layer and switch between feedstocks with significant differences. Solid insulators with graded permittivity are optimised through electric field distribution simulations and subsequently manufactured using our innovative multi-material SLA approach. A 4-layered graded insulator effectively decreases the maximum electric field strength from 82.5–30.8 kV/mm. Both flashover tests and partial discharge signals confirm that graded insulators outperform homogeneous ones in electrical insulation.

## ARTICLE HISTORY

Received 28 July 2023  
Accepted 10 October 2023

## KEYWORDS

Stereolithography 3D printing; high voltage insulators; graded permittivity composites

## 1. Introduction

Solid insulators are commonly used as electrical components to provide mechanical support and separate conductors [1]. However, in high voltage applications such as aerospace, military, and power grid transmission [2–4], the electric field distribution on the surface of solid insulators tends to be highly non-uniform. Especially, the maximum electric field strength ( $E_{\max}$ ) generated at the triple junction can lead to charge accumulation or partial discharge [5,6].

Based on the target of relaxing the electric field concentration, approaches including using corona rings, redesigning conductor shapes, or optimising insulator structures have been developed to modulate the electric field distribution in electrical devices [7–10]. Nevertheless, these conventional methods have increased structural complexity and manufacturing costs. In recent years, a novel concept involving graded permittivity insulators has emerged due to

their remarkable electric field relaxation effect in high voltage applications [1,2,11–14]. For instance, researchers have employed techniques like centrifugation, mixture casting, surface modification, and hot-pressing to create non-linear or graded permittivity insulators, effectively reducing high electric field strengths at critical points [2,15–25]. However, these methods fall short in manufacturing complex structures (e.g. hollow structures) and typically exhibit low processing efficiency. The application of 3D printing has created new possibilities for fabricating solid insulators with graded permittivity [26–31]. Among different 3D printing technologies, SLA stands out because it achieves an excellent balance between printing speed and precision [28,32,33]. Here, the graded materials can be in-situ synthesised layer by layer (the so-called multi-material SLA), providing precise control over the material composition of each layer [34,35].

**CONTACT** Guanghai Fei  [guanghai.fei@kuleuven.be](mailto:guanghai.fei@kuleuven.be)  Centre for Membrane Separations, Adsorption, Catalysis, and Spectroscopy (cMACS), KU Leuven, 3000 Leuven, Belgium

© 2023 The Author(s). Published by Informa UK Limited, trading as Taylor & Francis Group  
This is an Open Access article distributed under the terms of the Creative Commons Attribution-NonCommercial License (<http://creativecommons.org/licenses/by-nc/4.0/>), which permits unrestricted non-commercial use, distribution, and reproduction in any medium, provided the original work is properly cited. The terms on which this article has been published allow the posting of the Accepted Manuscript in a repository by the author(s) or with their consent.

Multi-material SLA 3D printing has found extensive use in the fabrication of graded materials [28,36–38]. However, a challenge in the field of multi-material SLA remains the development of novel strategies that can control printing parameters (exposure time and preset layer height) for every printing layer because most commercial SLA printers typically use a uniform set of parameters throughout the entire printing process, with no provision for parameter adjustments during printing [39]. Multi-material SLA, which involves different formulations, often requires longer exposure times and smaller layer heights when printing with scattering formulations that contain high permittivity fillers; conversely, a faster exposure process can be applied when creating parts using pure liquid resin or refractive index-matching suspensions [40]. The ability to achieve flexible, layer-level digital control over exposure time and layer height to accommodate a range of materials can significantly enhance the fabrication speed and increase the versatility of multi-material 3D printing.

Herein, we develop a multi-material and parameter-controllable SLA strategy to manufacture graded permittivity composites for high voltage insulators (Figure 1). To modify the material's permittivity, we have blended epoxy resin with BaTiO<sub>3</sub>, a dielectric ceramic commonly used in electrical insulation due to its high permittivity (>2000 at low frequencies <1 kHz) [41,42]. With this digital manufacturing strategy, we have achieved rapid and robust production of graded permittivity composites by employing different resin formulations (filled with varying amounts of BaTiO<sub>3</sub>) and applying layer-level digital control over exposure time and layer height. This process involves the preparation of printing files (slicing the 3D model into 2D patterns and assigning exposure times per layer) and multi-material SLA 3D printing (switching between different photocurable feedstocks). As a proof of concept, we have

manufactured various insulators with graded permittivity based on the electric field simulation analysis.

## 2. Materials and methods

An epoxy-acrylate-based resin (Esun3d Tech., Shenzhen, China) has been used as the matrix, which is sensitive to 405 nm light [40,43]. Commercially available BaTiO<sub>3</sub> particles (Aladdin Chemicals, Shanghai, China) were employed as fillers. The morphology of BaTiO<sub>3</sub> particles was taken by an S-4800 scanning electron microscope (HITACHI, Japan), while the particle size distribution was measured with a Malvern Zetasizer Nano ZS90 (Malvern Panalytical Ltd., UK). BYK dispersant (BYK-9076, BYK Chemie, Germany; further referred to as 'BYK') served as the surfactant for the particles. Composite feedstocks were formulated by mixing Esun resin with BaTiO<sub>3</sub> powders, followed by stirring at 800 rpm for 3 h at room temperature. The mixture was then degassed in a vacuum oven (20 mbar, room temperature) for 30 min. Subsequently, we measured the viscosity using a Brookfield viscometer (NDJ-1, LICHEN Tech., China) with the No. 4 spindle at a spinning rate of n = 12 rpm.

Electric field analysis and simulation were carried out based on a simplified model of a high voltage insulator. This simulation model includes high- and low-voltage electrodes, a cone-type insulator, SF<sub>6</sub> gas, and triple junctions on the insulator's surface. The simulation was based on material permittivity at 50 Hz, following IEC 62196–1 and IEC 60195:1965 standards. To ensure accuracy, we employed a high-resolution grid composed of triangular cells to define spatial sampling in the finite element model (FEM). In particular, we utilised the smallest mesh size, approximately 1 μm, around the triple junctions for the electric field analysis.

Before 3D printing, we exposed the feedstocks on a transparent substrate to a known dose of light and measured the resulting cured height using a digital

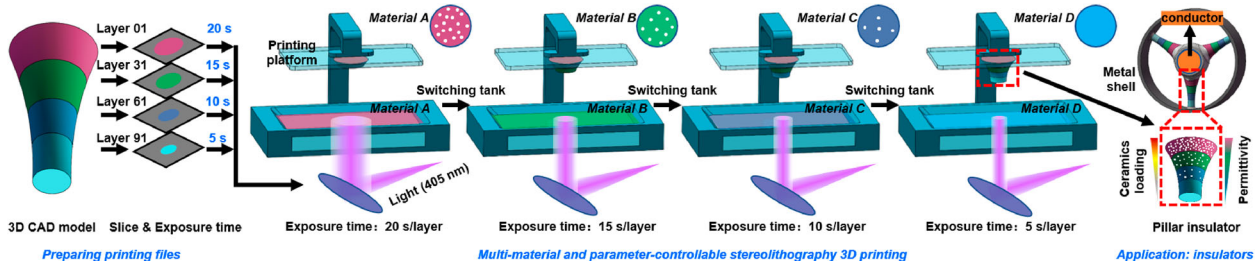


**Figure 1.** Multi-material and parameter-controllable SLA 3D printing of high voltage insulators. The process flow consists of preparing printing files (slicing the 3D model into 2D patterns and assigning exposure times per layer) and multi-material SLA 3D printing (switching between different photocurable feedstocks). The slice numbers and exposure times are indicative only. Formulations filled with different amounts of BaTiO<sub>3</sub> particles are used to modulate the resin properties, resulting in a composite print with a gradient in permittivity (right panel).

gauge (Awt-chy01, EVERTE Ltd., China). This process provided us with photopolymerization information and working curves for different formulations. We developed a custom SLA printing system that enables a multi-material 3D printing strategy, allowing us to assign different exposure times and layer height presets for each building layer. In our setup, the light source had a wavelength of 405 nm and an irradiation intensity of 2.5 mW/cm<sup>2</sup>. The projection area was approximately 130 mm × 80 mm, resulting in a pixel size of around 50 μm × 50 μm. Before manufacturing graded permittivity composites, we prepared different formulations with varying BaTiO<sub>3</sub> loadings. Multi-material SLA was achieved by mechanically switching the resin tank as the platform ascended. In the printing file, different building parameters (exposure time and preset layer height) were designed to accommodate different formulations. Besides, we incorporated an extra residence time for switching tanks after the platform ascended. Before printing a new material, we cleaned the existing cured SLA parts with ethanol.

The relative permittivity ( $\epsilon_r$ ) and dielectric loss ( $\tan\delta$ ) of cured samples (2 cm in diameter and 0.5 mm in thickness) with different BaTiO<sub>3</sub> ratios were measured using a dielectric impedance-thermal excitation current integrated analyzer (Concept 40, Novocontrol, Germany). The frequency dependence of the  $\epsilon_r$  and  $\tan\delta$  was tested from 10 Hz to 1 MHz at room temperature [44]. Flashover tests were conducted using a digitally controlled 100 kV non-PD (partial discharge) power supply (YUTW-10/100, Huasheng Tech., China). The voltage rise rate and discharge time interval were set to 0.2 kV/s and 180 s, respectively.

A modular partial discharge detector (DDX 9121b, HAEFELY HIPOTRONICS, Switzerland) equipped with an AKV 9310 measuring impedance was used to capture the discharge pulse and spectrum. The partial discharge detector included digital filters that enabled us to shift the measurement frequency band into a less noisy range and suppress frequency-dependent noise, thereby enhancing sensitivity.

### 3. Results and discussion

#### 3.1. Formulation and photopolymerization of BaTiO<sub>3</sub>-resin suspensions

To improve the electrical properties of the pure resin, BaTiO<sub>3</sub> has been introduced to the photocurable resin because of its high  $\epsilon_r$  [45]. Multi-sized BaTiO<sub>3</sub> particles (Figure 2a-b, 300–700 nm with a  $d_{50}=450$  nm) enable the formulation of stable and well-dispersed composite inks [46]. Since SLA is a light-based technique, we had

to address the strong scattering caused by the refractive index mismatch between BaTiO<sub>3</sub> particles (2.6) and the resin (1.5). Based on the modified Lambert-Beer law and scattering model [40], we mitigated this scattering effect by reducing the ceramic concentration in the resin matrix. Apart from photopolymerization, ceramic fillers typically increase the viscosity of the suspension, leading to poor processability [40,43]. We formulated a series of composite feedstocks to strike a balance between insulation performance and processability. These feedstocks were created by mixing Esun resin with BaTiO<sub>3</sub> particles at 10, 20, 30, 40, and 50 wt% concentrations.

The viscosity increases from around 200–760 mPa·s as the BaTiO<sub>3</sub> particle loading increases from 0 to 50 wt% (Figure 2c). BYK dispersant has been used to formulate suspensions with stable particle dispersion through steric stabilisation [43,45,47]. Several experiments have shown that the optimal BYK content usually falls between 3 and 7 wt% [31,45,48–51]. In this study, we expanded the range to 0–10 wt% to investigate the rheology of the printing suspensions. The viscosity was stable in suspensions with 4–8 wt% BYK content (Figure 2C).

When BaTiO<sub>3</sub> particles are present in the feedstock, the incident light is absorbed by the photoinitiators and scattered by the BaTiO<sub>3</sub> particles due to the refractive index mismatch with the resin matrix. As a result, the cure depth ( $C_d$ ) decreases with increasing solid loading (Figure 2d, cure depth: pure resin > 10 wt% > 20 wt% > 30 wt% > 40 wt% > 50 wt%). For instance, at an exposure time ( $t_0$ ) of 150 s, the  $C_d$  decreases from 700 (pure resin) to 70 μm (50 wt% BaTiO<sub>3</sub>-resin suspension). Based on Jacob's working curve equation [52], the reduction in cure depth by strongly scattering fillers can be offset by prolonging the exposure time ( $t_0$ ). Since light energy is the product of  $I \times t_0$  ( $I$  is light intensity), increasing the exposure time effectively boosts the exposure energy, thereby increasing the cure depth. For instance, to achieve a cured height of 50 μm, the required exposure times for different suspensions are as follows: 6 s (pure resin), 8 s (10 wt%), 12 s (20 wt%), 20 s (30 wt%), 38 s (40 wt%), and 60 s (50 wt%).

$$C_d = D_p \times \ln \frac{E_0}{E_c} = D_p \times \ln \frac{I \times t_0}{I \times t_c} \quad (1)$$

where  $C_d$  (the cure depth) is linearly proportional to the logarithm of  $E_0$  (the incident light energy),  $D_p$  is the penetration depth related only to the properties of the printing materials and  $E_c$  is the critical energy of light curing (the minimum exposure energy required to initiate polymerisation).

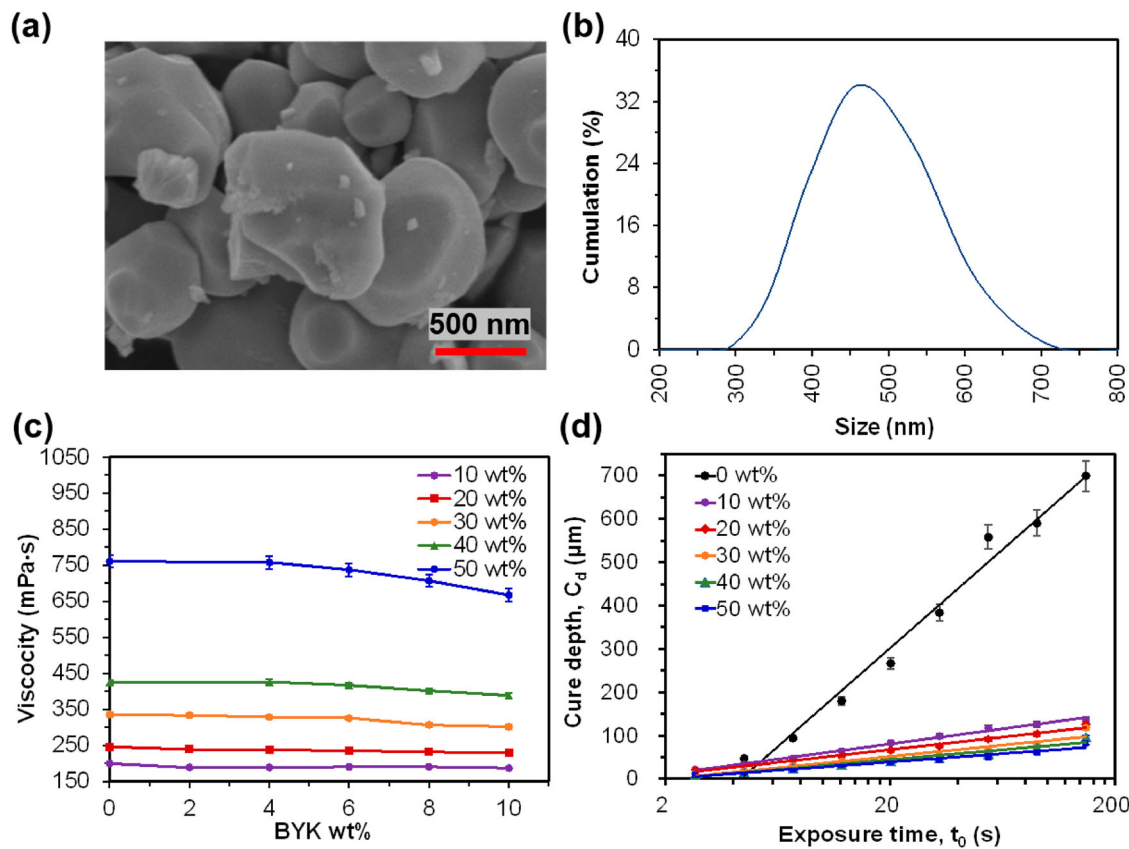


**Figure 2.** Formulation and photopolymerization of BaTiO<sub>3</sub>-resin suspensions. **(a)** Morphology of BaTiO<sub>3</sub> particles. **(b)** Particle size distribution of BaTiO<sub>3</sub>. **(c)** The viscosity of BaTiO<sub>3</sub>-resin suspensions. **(d)** SLA working curves, plotted with different measured cure depths.

### 3.2. Electrical properties of BaTiO<sub>3</sub>-resin composites

The electrical properties of different 3D-printed BaTiO<sub>3</sub>-resin composites were studied, including the relative permittivity ( $\epsilon_r$ ), the dielectric loss ( $\tan\delta$ ), and the flashover properties. Compared to pure resin, the  $\epsilon_r$  of BaTiO<sub>3</sub>-resin composites increases with the BaTiO<sub>3</sub> concentration (Figure 3a-b). For example, at 50 Hz, the  $\epsilon_r$  of 50 wt% BaTiO<sub>3</sub>-resin composite reaches 26.5, approximately six times that of pure resin (around 4.5). Similarly, the  $\tan\delta$  of BaTiO<sub>3</sub>-resin composites increases with the BaTiO<sub>3</sub> concentration (Figure 3c), which is caused by the substantial differences in dielectric properties (polarizability and conductivity) between the filler and matrix [53,54]. It's worth noting that due to adequate polarisation [55], the  $\epsilon_r$  and  $\tan\delta$  are relatively high at low frequency (< 1 kHz). Subsequently, we conducted flashover tests at varying air pressures (ranging from 0.1–0.3 MPa). The flashover voltage does not exhibit significant variation with changes in BaTiO<sub>3</sub> concentration. However, it increases from approximately 11–20 kV as the air pressure rises from 0.1–0.3 MPa (Figure 3d).

### 3.3. Simulation of the electric field distribution in different insulators

A simplified simulation model of a graded insulator is shown in Figure 4a-c. In the case of homogeneous insulators (pure resin and 25, 50 wt% BaTiO<sub>3</sub>-resin composites), the electric field strength ( $E$ ) decreases from point B (high voltage electrode) to C (low voltage electrode). However, for graded insulators with 2, 3, or 4 layers, the descending curve exhibits multiple convex values at the interfaces between materials with different permittivity (Figure 4d). We optimised the permittivity values of the multi-layers in graded insulators, simulating values ranging from 4.5–30 with an increment of 0.5. For example, in the case of the 3-layered insulator, the optimal permittivity for the middle layer is 8.5. In the 4-layered insulator, the optimal combination ranges from 26.5–10, 6, and 4.5 (from point B to point C). The maximum electric field strength ( $E_{max}$ ) generated in electrical insulating components is critical, as it is linked to partial discharge or charge accumulation issues. In this study,  $E_{max}$  at the triple junction decreased from 82.5–30.8 kV/mm when transitioning from a composite filled with 50 wt% BaTiO<sub>3</sub> to the 4-layered graded permittivity composite.

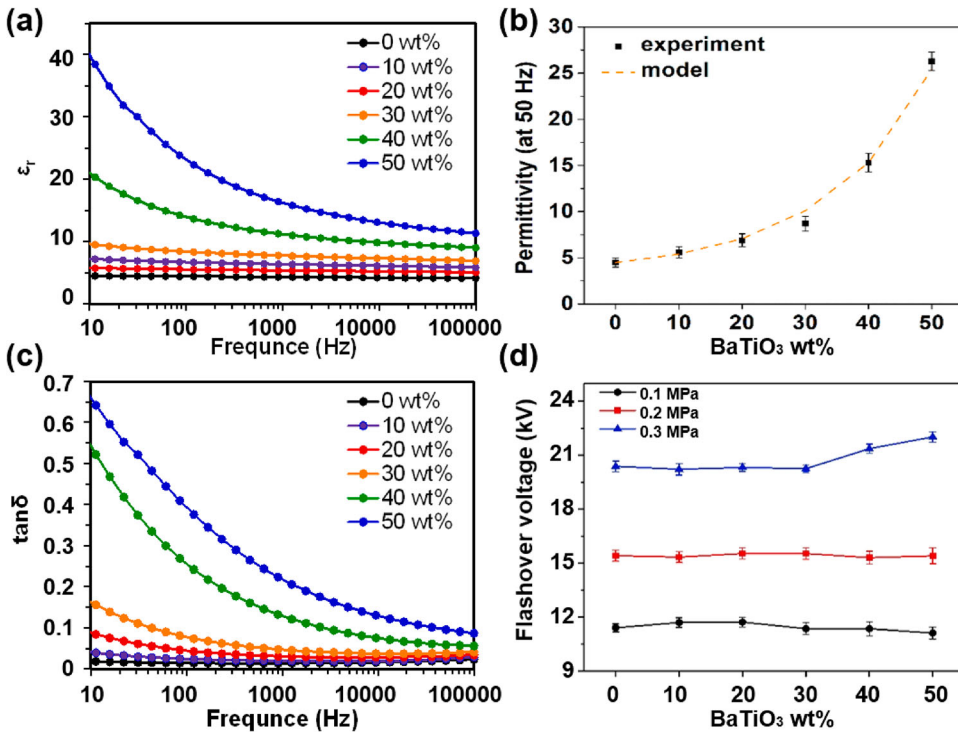
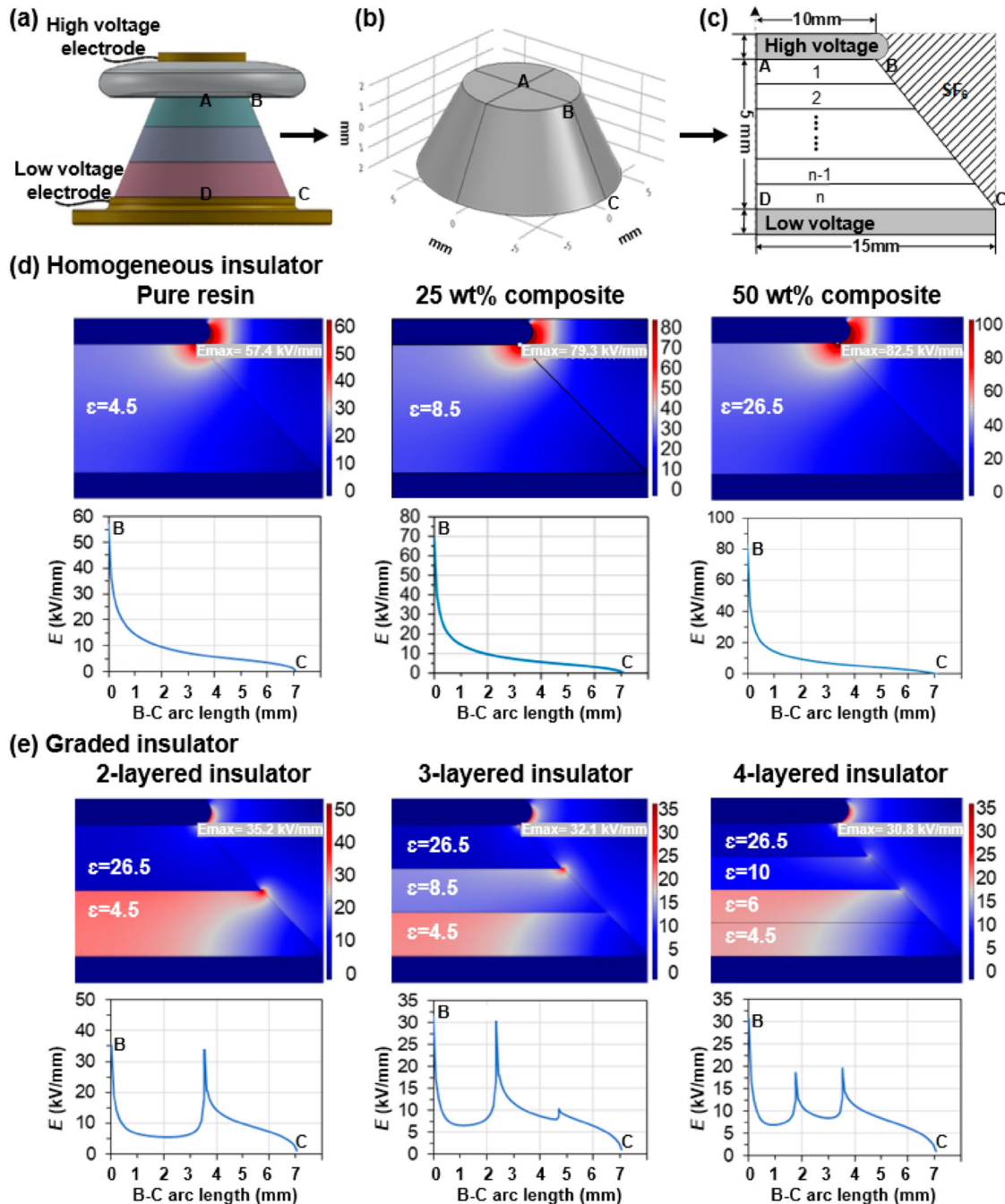


**Figure 3.** Electrical properties of BaTiO<sub>3</sub>-resin composites. **(a)** Frequency dependence of permittivity. **(b)** Permittivity of BaTiO<sub>3</sub>-resin composites at 50 Hz (experiment and prediction value): the prediction model is the Lichtenecker logarithmic law of mixing [56]. **(c)** Frequency dependence of dielectric loss. **(d)** Flashover voltage of BaTiO<sub>3</sub>-resin composites at different air pressures (0.1–0.3 MPa).

The  $E_{\max}$  generated at the triple junction (high voltage conductor – insulator – SF<sub>6</sub> gas; red points in Figure 5a, b) directly depends on the applied voltage and the surface charge density mismatch between the insulator and SF<sub>6</sub> gas. To understand the mechanism behind  $E_{\max}$  generation, we have to consider two scenarios: homogeneous insulators (Figure 5a) and graded insulators (Figure 5b). In the case of homogeneous insulators, where the insulators with the same applied voltage ( $\mathbf{U}$ ), the insulator surface charge density increases ( $\sigma_a < \sigma'_a < \sigma''_a$ ) as the permittivity rises from 4.5–26.5. Consequently,  $E_{\max}$  increases when transitioning from pure resin to BaTiO<sub>3</sub>-filled composite (pure resin < 25 wt% BaTiO<sub>3</sub> < 50 wt% BaTiO<sub>3</sub>). For graded insulators, as we increase the types of heterogeneous materials (from 2 to 4), the voltage decreases ( $\mathbf{U}_1 > \mathbf{U}_3 > \mathbf{U}_6$ ) because the graded materials can uniform the voltage distribution. This voltage distribution further leads to a decrease in surface charge density ( $\sigma_b > \sigma'_b > \sigma''_b$ ). As a result,  $E_{\max}$  decreases when transitioning from 2-layered to 4-layered insulators (4-layered < 3-layered < 2-layered). In direct comparisons between graded and homogeneous insulators, graded permittivity materials consistently yield lower  $E_{\max}$  values due to their ability to uniform voltage distribution.

### 3.4. Multi-material SLA of graded insulators and their electrical properties

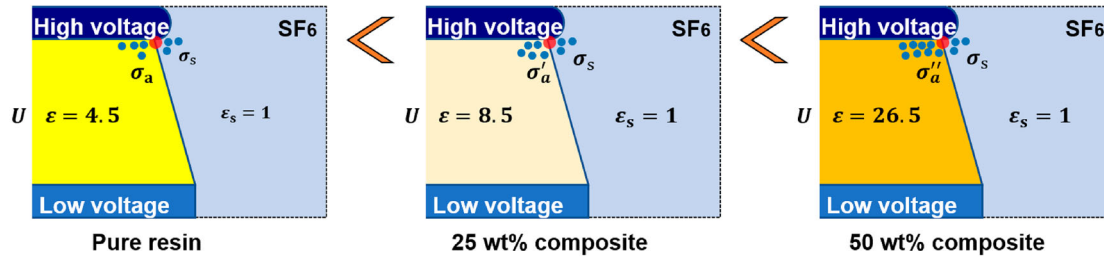
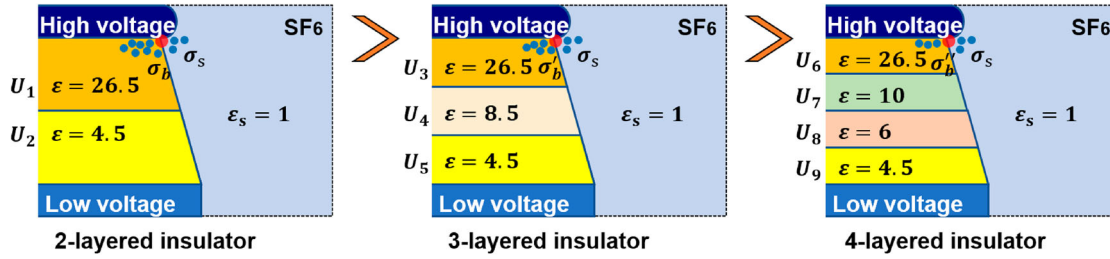
We successfully fabricated insulators with graded permittivity using multi-material SLA 3D printing technology based on the simulation results. As an illustrative example, we simulated the optimal permittivity combination for the 4-layered insulator: 26.5-10-6-4.5 (Figure 4d), which combination corresponds to composites filled with 0, 13, 33, and 50 wt% BaTiO<sub>3</sub> (Figure 3b). For different BaTiO<sub>3</sub>-filled suspensions, the reduction in cure depth by strong scattering can be offset by either prolonging the exposure time or reducing the layer height [42,57]. Conversely, pure resin enables acceleration of the build process as it can be cured with a short exposure time. As a result, we designed dynamic digital exposure strategies for different suspensions and insulators (Table 1). Taking the 3-layered insulator as an example (Figure 6a), different printing parameters were designed for different formulations: Material **A** (Pure resin) – layer height: 50 μm/layer, exposure time: 6 s/layer; Material **B** (Composite filled with 25 wt% BaTiO<sub>3</sub>) – layer height: 10 μm/layer, exposure time: 16 s/layer; Material **C** (Composite filled with 50 wt% BaTiO<sub>3</sub>) – layer height: 10 μm/layer, exposure time: 30 s/layer.



**Figure 4.** Simulation of the electric field distribution in different insulators. **(a-c)** Simplified simulation model of a graded insulator. **(d-e)** Electric field distribution in different insulators. **(d)** For the homogeneous insulators, the permittivity value is set to 4.5, 8.5 and 26.5 (the measurement value of pure resin and composites at 50 Hz). **(e)** For the graded insulators, the permittivity value of the multi-layers is optimised by simulating different values ranging from 4.5–30 (with an increment of 0.5).

Using different formulations and building parameters, we printed different insulators (Figure 6b). After the 3D-printed insulators were post-cured and dried, flashover tests were conducted to evaluate their insulation performance. The flashover voltage was found to increase as air/SF<sub>6</sub> pressure increased. It's worth noting that the flashover voltage is higher in the SF<sub>6</sub> condition than in the air (Figure 6c-d), indicating

that the 3D-printed insulators operate better in the SF<sub>6</sub> condition. By optimising dielectric parameters and using gradient materials, the electric field distribution at the gas–solid interface becomes more uniform. As a result, graded insulators exhibit enhanced flashover properties, enabling discharge to occur at higher voltages. The performance of different insulators is similar to the simulation results, where the 4-layered and

**(a) Case 1: homogeneous insulator****(b) Case 2: graded insulator**

**Figure 5.** The generation mechanism of maximum electric field strength ( $E_{\max}$ ) at the triple junction. **(a)** Homogeneous insulators. **(b)** Graded insulators.

3-layered graded insulators outperform the 2-layered graded insulators and pure resin insulators. Conversely, the insulator with a composite filled with 50 wt% BaTiO<sub>3</sub> performs the poorest.

When high voltages are applied, the high electric field generated in the electrical insulating components might cause partial discharge or sudden electrical breakdown [58,59]. In this study, we collected partial discharge signals from various insulator samples tested at 6 and 9 kV with a frequency of 50 Hz. Compared to the homogeneous insulators (pure resin and composite filled with BaTiO<sub>3</sub>), graded insulators exhibited a reduction in the amplitude of partial discharge, resulting in improved

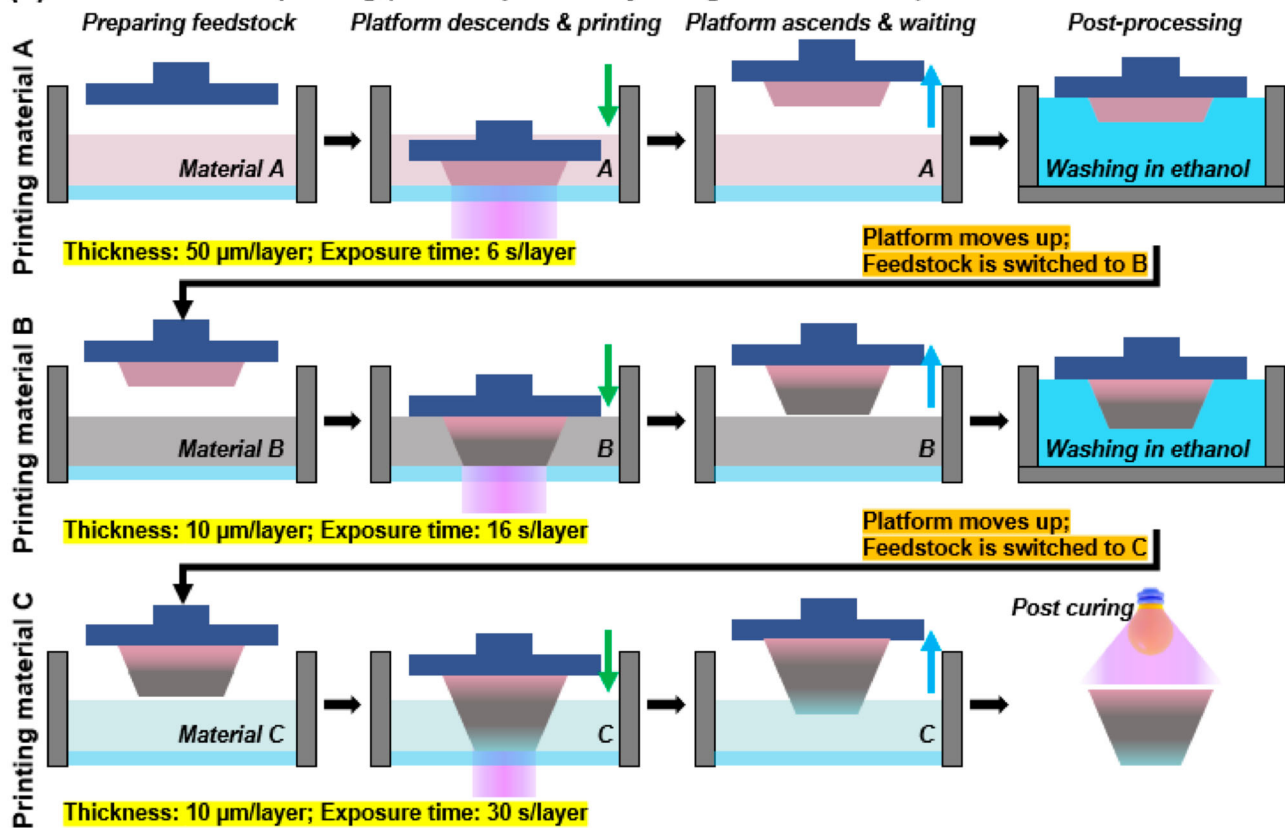
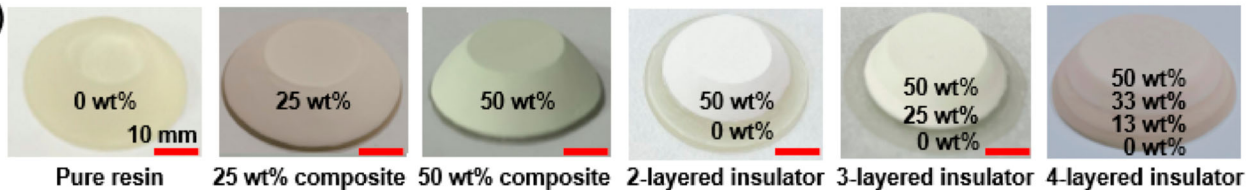
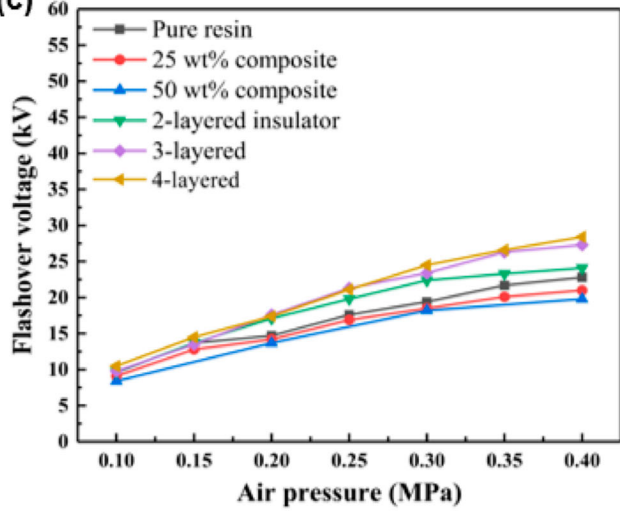
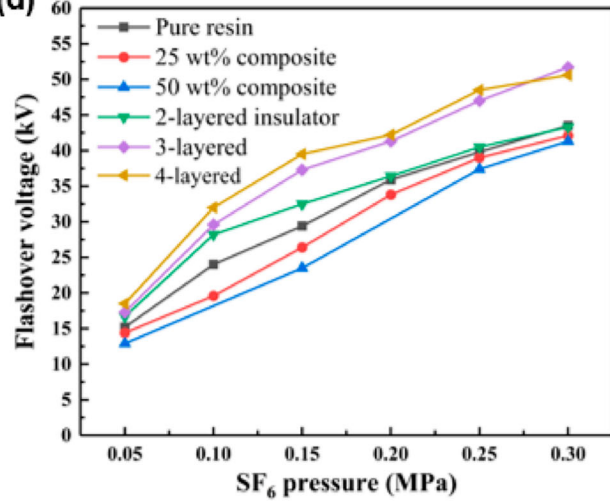
performance in terms of average and maximum partial discharge values (Figure 7). Regarding the performance of graded insulators, it's worth noting that the 4-layered insulator does not demonstrate a significant advantage over the 2-layered or 3-layered insulator. For instance, at a test voltage of 9 kV, the maximum partial discharge values for different graded insulators were as follows: 10697 pC (2-layered), 9975 pC (3-layered), and 8895 pC (4-layered). Similarly, the average partial discharge values for these graded insulators were 150 pC (2-layered), 125 pC (3-layered), and 100 pC (4-layered). These insights inform the design and manufacturing of graded insulators, helping to strike a balance between the final device's functionality and the complexity of the manufacturing process.

**Table 1.** Printing parameters for different suspensions and graded insulators.

Suspensions	Permittivity ( $\epsilon$ ) at 50 Hz	Layer height/layer ( $\mu\text{m}$ )	Exposure time/layer (s)
Pure resin	4.5	50	6
Composite filled with 13 wt% BaTiO <sub>3</sub>	6	20	12
Composite filled with 25 wt% BaTiO <sub>3</sub>	8.5	10	16
Composite filled with 33 wt% BaTiO <sub>3</sub>	10	10	20
Composite filled with 50 wt% BaTiO <sub>3</sub>	26.5	10	30
Graded insulators	Permittivity ( $\epsilon$ ) at 50 Hz	Layer height/layer ( $\mu\text{m}$ )	Exposure time/layer (s)
2-layered insulator (50 wt%, resin)	(26.5, 4.5)	(10, 50)	(30, 6)
3-layered insulator (50, 25 wt%, resin)	(26.5, 8.5, 4.5)	(10, 10, 50)	(30, 16, 6)
4-layered insulator (50, 33, 13 wt%, resin)	(26.5, 10, 6, 4.5)	(10, 10, 20, 50)	(30, 20, 12, 6)

### 3.5. Benchmark study and perspectives

Various technologies have been employed to fabricate graded permittivity composites. Notably, methods such as flexible mixture casting, surface modification, hot-pressing, and 3D printing have shown significant potential in modulating electric field distribution and improving surface flashover performance (Table 2). The multi-material SLA 3D-printed graded permittivity composite shows good electrical performance comparable to other methods. Most techniques reduce the maximum electric field by >50% and increase the flashover voltage by >40%. In comparison to casting and surface modification, 3D printing methods, especially fused deposition modelling (FDM) and SLA, have emerged as promising alternatives for crafting

**(a) Multi-material 3D printing (an example of 3-layered graded insulator)****(b)****(c)****(d)**

**Figure 6.** Multi-material SLA of different insulators and their flashover properties. **(a)** 3D printing process flow (an example of the 3-layered insulator). **(b)** 3D-printed insulators. **(c-d)** Flashover properties of different insulators at different air pressures (air: 0.1–0.4; SF<sub>6</sub>: 0.05–0.3).

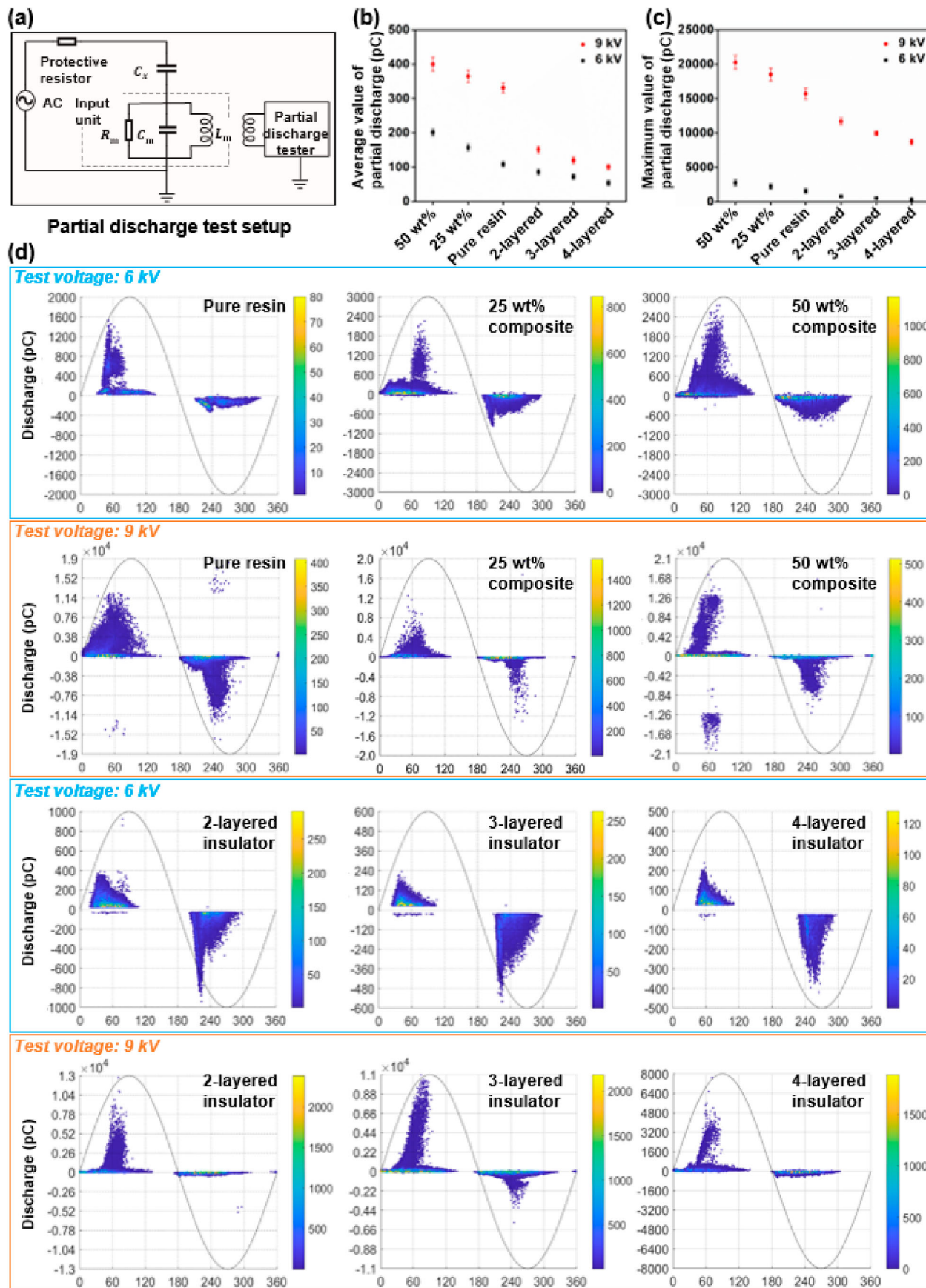


**Figure 7.** Partial discharge tests for different insulators. **(a)** Partial discharge test setup. **(b)** Average and **(c)** maximum values of partial discharge. **(d)** Partial discharge signals of the samples at different voltages (6 and 9 kV with a frequency of 50 Hz).

**Table 2.** Comparison of different insulation materials/structures.

Insulation materials	Manufacturing	Performance improvements	Drawbacks
Functionally graded spacer [2,15,16]	Casting / flexible mixture casting	Varying permittivity: 4–30; maximum electric field reduced by 64%; discharge inception voltage improvement: 70% higher	<ul style="list-style-type: none"> <li>Layer-by-layer casting</li> <li>Fall short in manufacturing complex structures (e.g. hollow structure)</li> </ul>
Graded permittivity materials [17,18]	Centrifugation method	Materials with various permittivity: from 3.6–6.4	<ul style="list-style-type: none"> <li>Fall short in manufacturing complex structures</li> <li>Inconvenient to control the permittivity of local region</li> </ul>
Graded materials [19–23]	Surface modification: coating; magnetron sputtering; plasma	Maximum electric field reduced by 70%; surface flashover voltage increased from 25.9–33.8 kV	<ul style="list-style-type: none"> <li>Only the surface layer with different permittivity material</li> <li>Low processing efficiency</li> </ul>
Permittivity-gradient multilayer organic composite [24,25]	Assemble + hot-pressing	Surface flashover voltage is increased by 75%	<ul style="list-style-type: none"> <li>Insulators with non-continuous gradient</li> <li>Fall short in manufacturing complex structures</li> </ul>
Non-uniform insulator [13,60,61]; multilayered cylindrical dielectric lens antenna [26]; composites with anisotropic dielectric properties [27]	Fused deposition modelling (FDM) 3D printing	Varying dielectric constant: 3.3–13.4; surface flashover voltage increased by 41%	<ul style="list-style-type: none"> <li>Interior defects (voids) in FDM parts</li> <li>High thermal expansion coefficient of printed polymer</li> </ul>
Composite filled with alumina [62]; 2-layered permittivity-graded resin/alumina composite [28]	SLA 3D printing	Permittivity at 1 MHz increased from 3.8 (unfilled epoxy) to 5.6 (40% alumina composite)	The permittivity is still small
Composite filled with BaTiO <sub>3</sub> nanowires [63] or BaTiO <sub>3</sub> microspheres [42] or modified PZT nanoparticles [64] or cellulose nanocrystals [65]	SLA 3D printing	Dielectric constant increased from 4 to 120 at 100 Hz (PZT); and from 3 to 15.3 at 50 Hz (BaTiO <sub>3</sub> nanowires)	Homogeneous composite
Graded permittivity composites [29–31]	Magnetic/electric field-assisted fabrication (3D printing)	Breakdown voltage improved by 70% (to pure epoxy) and 30% (to homogeneous composite)	<ul style="list-style-type: none"> <li>Difficult in large-scale and complex-shaped structures</li> <li>Inconvenient to control the permittivity of local regions</li> </ul>
Graded permittivity composites (this study)	Multi-material SLA 3D printing	Permittivity at 50 Hz increased from 4.5–26.5 (around 6 times); maximum electric field strength decreased from 82.5–30.8 kV/mm (around 3 times); flashover voltage increased from 20 to 30 kV in the air (by 50%)	Insulators with non-continuous gradient

graded permittivity materials due to the high degree of design freedom and highly efficient production. Specifically, SLA stands out when high-resolution and filled feedstock is required.

Theoretically, the present multi-material SLA technique can allocate distinct material compositions for each printed layer, potentially achieving a continuous gradient in BaTiO<sub>3</sub> content ranging from 0% to 50 wt %. However, pursuing this approach is deemed unnecessary as the 4-layered insulator in this study does not exhibit a significant advantage over the 3-layered insulator regarding flashover and partial discharge properties. When evaluating the marginal improvement in performance against the drawbacks – such as prolonged building time and heightened manufacturing complexity due to formulating multiple feedstocks before printing and increasing waiting times during tank switching – a more prudent strategy

would involve designing and fabricating materials with suitable gradient levels tailored to specific applications rather than pursuing continuous graded permittivity materials.

#### 4. Conclusion

A multi-material and parameter-controllable SLA 3D printing strategy that can assign different exposure times and layer height presets for each building layer is developed to fabricate graded permittivity composites for high voltage insulators. The 3D-printed graded insulators outperform homogeneous ones, as confirmed through simulations, flashover tests, and partial discharge signals. When considering the balance between device functionality and manufacturing complexity, it becomes clear that designing insulators with tailored gradient levels for specific applications is a more





